

IMECE2015-50977

**STABILITY ANALYSIS OF A MACROSCOPIC TRAFFIC FLOW MODEL FOR
ADAPTIVE CRUISE CONTROL SYSTEMS**

K.N. PORFYRI

Technical University of Crete, School of Production
Engineering and Management,
University Campus, GR-73100, Chania, Greece
kporfyri@dssl.tuc.gr

I.K. NIKOLOS¹

Technical University of Crete, School of Production
Engineering and Management,
University Campus, GR-73100, Chania, Greece
jnikolo@dpem.tuc.gr
¹Contact Author

A.I. DELIS

Technical University of Crete, School of Production
Engineering and Management,
University Campus, GR-73100, Chania, Greece
adelis@science.tuc.gr

M. PAPAGEORGIU

Technical University of Crete, School of Production
Engineering and Management,
University Campus, GR-73100, Chania, Greece
markos@dssl.tuc.gr

ABSTRACT

Since the early days of traffic engineering, traffic flow stability has attracted a lot of attention, as the frequent occurrence of traffic jams, caused by small perturbations in traffic flow such as a sudden deceleration of a vehicle, deteriorate the performance of traffic flow and the utilization of the available infrastructure. Such traffic jams are usually related to instabilities in traffic flow, resulting in the formation of stop-and-go waves, propagating upstream the traffic flow. Emerging technologies in the field of Vehicle Automation and Communication Systems (VACS), such as Adaptive Cruise Control (ACC) systems, appear to be a remedy to reduce the amplitude or to eliminate the formation of such traffic instabilities. To this end, this work aims to derive a stability threshold of a novel macroscopic model, developed to simulate the flow of ACC-equipped vehicles, and study the impact of such vehicles on the stabilization of the traffic flow, with respect to small perturbations. The adopted macroscopic approach reflecting ACC traffic dynamics is based on the gas-kinetic (GKT) traffic flow model. The analytic results show that ACC vehicles enhance the stabilization of the traffic flow; the instability region is very narrow and by reducing the ACC time-gap setting it moves to higher values of density.

Keywords: Linear stability analysis, macroscopic traffic flow modeling, Adaptive Cruise Control.

1. INTRODUCTION

Vehicle Automation and Communication Systems (VACS), and the related technologies involved in their development, are expected to radically change the way traffic flow will be controlled. Systems such as Adaptive Cruise Control (ACC) ones, have been initially developed to increase driver's comfort and passengers' safety. However, they have an additional effect on reducing the amplitude or eliminating the formation of traffic flow instabilities, for specific values of their parameters. This characteristic, along with the expected spreading of such systems, can provide additional tools for the solution of the continuously increasing problem of traffic congestion.

ACC systems allow vehicles to follow each other automatically, using as input parameters the time gap to the vehicle immediately in front of it -referred to as the leader-, the speed difference, and the speed of the equipped vehicle. The braking system forces the equipped vehicle to slow down when the leader drives with a lower speed, while, on the other hand, the vehicle accelerates towards the pre-set speed limit when the leader accelerates or is out of the range of the equipped vehicle's sensors. Thus, by relieving the driver from continuous speed adjustments to the speed of the leader, the ACC systems are potentially able to considerably increase driving comfort and prevent collisions. Remarkably, even though ACC systems promise substantial benefits in comfort and safety in various driving situations, may have adverse impacts on the performance and stability of traffic flow, under specific settings of their controlling parameters. Hence, from the traffic management

point of view, in order to ensure that such systems will be developed and implemented in ways to improve rather than deteriorate traffic flow conditions, it is desirable to assess their effects on traffic flow dynamics, by appropriate modelling and simulation. In a second level, such modelling and simulation tools can be used for the optimization of the settings of ACC systems, to optimize their performance, with respect not only to the comfort and safety, but also to the traffic flow dynamics.

Towards this direction, the derivation of stability criteria to characterize the influencing factors of traffic flow instabilities and identify the way that ACC systems affect traffic flow stability is an important issue, which should be taken into consideration. Indeed, as pointed out in [1], in cases where the ACC systems are unable to ensure string or traffic flow stability, traffic safety and congestion may be aggravated rather than improving. In general, traffic instabilities relate to the occurrence of traffic jams, resulting in the formation of stop-and-go waves, which propagate upstream against the traffic flow. The occurrence of instabilities in traffic flow has been the subject of many studies since 1950s [2]. In literature, both linear and nonlinear stability methods have been applied widely in order to derive stability conditions, using either microscopic models [2–16] or macroscopic ones [3, 8, 10, 16–29]. It is necessary at this point to clarify that the stability analysis obtained from macroscopic models is called flow stability, referring to the way density and speed evolve in response to the perturbations caused by the decrease or increase of the downstream density or speed. On the contrary, the stability analysis based on microscopic models refers to the string stability of a platoon of vehicles following each other, describing how the disturbances from the deceleration of the leading vehicles are propagated to the following ones [16, 30]. For a more detailed review of the different categories of traffic flow models, as well as the general stability methods for each category, we refer to [16].

A wide range of microscopic approaches have been reported in the literature that deal with simulating the behavior of individual vehicles in the presence of ACC systems [31–38], analyzing simultaneously linear or nonlinear instabilities of traffic flow, in order to evaluate the impact of the penetration of such systems on traffic dynamics [39–48]; on the other hand, analogous model applications of macroscopic or gas kinetic traffic flow models are relatively limited. Nevertheless, as macroscopic traffic flow models generally call for less computational demand and simpler calibration and validation effort than microscopic ones, the development of macroscopic models for the near real-time simulation of ACC traffic will be of great importance in the future.

Swaroop and Rajagopal [30] studied the traffic flow stability under an ACC spacing policy, using an aggregated macroscopic traffic flow model for an open stretch highway with entries and exits. Using a linearized stability analysis they concluded that the traffic flow equilibrium state was marginally stable, but traffic flow was unstable when using spatially discretized stability analysis for a constant time headway (CTH) policy. In [49] the existing Payne macroscopic model was extended to consider the impact of ACC systems on traffic flow. Simulation results

showed that at lower time headways the traffic flow rate is increasing and the congestion is vanished faster, even with small penetration rates; until a certain penetration rate (30%) the traffic flow rate is increasing whereas a further increase of the penetration rate does not bring a substantial gain. Moreover, in [50] a macroscopic model was proposed with velocity saturation representing both the spatially biasing strategy and ACC-equipped vehicle dynamics. Additionally, a nonlinear traffic flow stability criterion, using a wavefront expansion technique, was derived, resulting in both necessary and sufficient conditions for the prediction of ACC traffic flow stability. Finally, Ngoduy proposed an extended multiclass gas-kinetic theory, taking into consideration the effects of ACC vehicles [51]. Using the linear stability analysis, it was shown that ACC vehicles stabilize traffic flow with respect to a small perturbation; the numerical simulations of the developed model indicated that increasing the penetration of ACC vehicles ensures more stable traffic flow.

The present work aims to derive a stability threshold of a new second-order macroscopic model, developed to simulate the flow of ACC-equipped vehicles, and study the impact of such vehicles on the stabilization of the traffic flow, with respect to small perturbations. The proposed model has been developed based on the gas-kinetic-based traffic flow (GKT) model, with the effects of ACC-equipped vehicles taken into consideration by proper adaptations.

2. THE GKT MODEL FOR ACC SYSTEMS

The application of gas-kinetic models has attracted continuously increasing interest during the past years [26, 51–55], bridging the gap between macroscopic and microscopic ones by obtaining aggregate traffic flow variables from a microscopic model with explicit consideration of vehicle-driver dynamics. Towards this direction, a novel second-order macroscopic approach was derived to incorporate the behavior of ACC equipped vehicles into the GKT model. In the latter, the macroscopic traffic flow equations are derived from the gas-kinetic ones using the method of moments [22, 51, 53, 56–58]. The resulting partial differential equations contain a non-local term instead of a diffusion one, which has favorable properties regarding the robustness of numerical integration methods and integration speed. Therefore, this model allows for a robust real-time simulation even in case of extended freeway networks in reasonable computational times [53]. Moreover, the GKT model is able to describe the hysteretic phase transitions to congested states, the so-called “synchronized traffic”, which is the most frequent form of congested traffic, typically occurring behind on-ramps, gradients, or other bottlenecks of busy highways [59, 60].

In the remainder of this section, we recall the GKT model incorporating the behavior of ACC vehicles. Denoting by $\rho(x, t)$ the traffic density (number of vehicles per unit length) as a function in space, x , and time, t , $u(x, t)$ the average speed of vehicles and $q(\rho, u) = \rho(x, t)u(x, t)$ the traffic flow rate (number of vehicles per unit of time), the reformulated GKT model in conservation law (balance law) form is written as

$$\partial_t \rho + \partial_x(\rho u) = 0 \quad (1)$$

$$\begin{aligned} \partial_t(\rho u) + \partial_x(\rho u^2 + \theta \rho) = \\ \rho \left(\frac{V_e^*(\rho) - u}{\tau} \right) [1 - \beta F(\rho)] - \alpha V_{acc} \end{aligned} \quad (2)$$

In the momentum dynamics Equation (2), the terms of αV_{acc} and $[1 - \beta F(\rho)]$, have been incorporated to model the behavior of ACC vehicles. The pressure-like term θ is a density-dependent fraction $A(\rho)$ of the squared velocity $\theta = A(\rho)u^2$, where $A(\rho)$ is the Fermi function

$$A(\rho) = A_0 + \delta A \left[1 + \tanh \left(\frac{\rho - \rho_{cr}}{\delta \rho} \right) \right] \quad (3)$$

in which ρ_{cr} is the critical density for the transition from free flow to congested traffic and $\delta \rho$ is the width of the transition region. Typical range of values for the constants $\delta \rho$, A_0 , and δA are given in Table 1, along with other model parameters taking into account [16, 51, 53, 54, 61, 62].

The dynamic equilibrium speed $V_e^*(\rho) = (\rho, u, \rho_\alpha, u_\alpha)$, which depends on the local (ρ, u) and the non-local traffic state (ρ_α, u_α) , is determined as

$$\begin{aligned} V_e^*(\rho) = (\rho, u, \rho_\alpha, u_\alpha) = \\ u_{max} \left[1 - \frac{\theta + \theta_\alpha}{2A\rho_{max}} \left(\frac{\rho_\alpha T}{1 - \rho_\alpha/\rho_{max}} \right)^2 B(\delta u) \right] \end{aligned} \quad (4)$$

The non-local traffic state (ρ_α, u_α) is computed at the interaction location $x_\alpha = x + \gamma(1/\rho_{max} + T \cdot u)$, with T being the desired time gap and γ a scale parameter. Finally, the Boltzmann (interaction) factor B that contains the standard normal distribution and the Gaussian error function, is defined as

$$B(z) = 2 \left[z \frac{e^{-z^2/2}}{\sqrt{2\pi}} + (1 + z^2) \int_{-\infty}^z \frac{e^{-y^2/2}}{\sqrt{2\pi}} dy \right] \quad (5)$$

This monotonically increasing term describes the dependence of the braking interaction on the dimensionless velocity difference δu , with $\delta u = \frac{u - u_\alpha}{\sqrt{\theta + \theta_\alpha}}$, between the actual position x and the interaction point x_α .

Compared to other macroscopic traffic flow models, the GKT model has the additional property to take into consideration the nonlocal interaction term in the velocity Equation (4). Although this nonlocality has smoothing attributes similar to those of a diffusion or viscosity term, its effect is more realistic as it is forwardly directed, implying that vehicles react on density or velocity gradients in front of them [53]. Moreover, in contrast to other macroscopic models, the steady-state (equilibrium) speed-density relation, $V^e(\rho)$, is implicitly given from the steady-state condition on homogeneous roads,

$$V^e(\rho) = \frac{\tilde{u}^2}{2u_{max}} \left(-1 + \sqrt{1 + \frac{4u_{max}^2}{\tilde{u}^2}} \right) \quad (6)$$

where:

$$\tilde{u} = \frac{1}{T} \left(\frac{1}{\rho} - \frac{1}{\rho_{max}} \right) \sqrt{\frac{A(\rho_{max})}{A(\rho)}} \quad (7)$$

The developed modified model for the macroscopic simulation of ACC traffic was incorporated as a source term to the momentum equation of the GKT model, which controls the speed dynamics, contributing to the relaxation term in the GKT model equations and also taking explicitly into account the important for ACC systems time-gap parameter. More specifically, this is done through the terms αV_{acc} and $[1 - \beta F(\rho)]$ of the Equation (2), where by setting $\alpha = \beta = 1$ the ACC approach is obtained, while for $\alpha = \beta = 0$ the manual driving is modeled, as the original GKT model describes.

Parameters	Units	Typical values
Desired free speed, u_{max}	km/h	[110,130]
Maximum density, ρ_{max}	veh/km	[140,160]
Critical density, ρ_{cr}	veh/km	[0.25, 0.4] ρ_{max}
Desired time gap, T	s	[1, 2]
Anticipation factor, γ		[1, 2]
Relaxation time, τ	s	[20, 40]
Variance pre-factor for free traffic, A_0		0.008
Pre-factor δA		$2.5A_0$
Transition width $\delta \rho$	veh/km	[0.05, 0.1] ρ_{max}

Tab. 1: Typical range of the parameters used for the GKT model.

At this point, it is essential to highlight that the proposed approach is based on the following necessary control objectives for ACC vehicles, according to [63]:

- *Speed control mode:* to travel at a user-set maximum velocity in cases where the radar or other sensors do not detect leading vehicles, or leading vehicles are detected but their speeds are higher than the pre-set maximum velocity.
- *Gap control mode:* to retain vehicle velocity equal to the velocity of the leading vehicle so as to ensure the specified spacing, in cases where the leading vehicle is detected by the radar or other sensors and its velocity is lower than the user-set maximum speed
- Transitions between the two aforementioned control objectives should be as smooth as possible, in order to avoid the inconvenience of the passengers, on account of sudden changes of velocity or abrupt maneuvers.

Time/space-headway is the time/space interval between the front bumpers of successive vehicles, while *time/space-gap* is

the time/space interval between the rear and front bumpers [16]. A popular control policy is the Constant Time Headway (CTH) policy whereby the inter-vehicle spacing is a linear function of the vehicle's speed [1]; this type of ACC policy was adopted for the proposed model. The following assumptions were adopted for the developed model in order to implement the aforementioned objectives:

- I. In cases where the density is explicitly less than a threshold ρ_{acc} (lower than or equal to the critical density ρ_{cr}) there is limited or no influence of the additional term to the GKT model, since it is supposed that the drivers react by setting their maximum desired speeds. For density values around ρ_{acc} a smooth but fast transition between the manual case and the ACC model is established, using the Fermi function:

$$F(\rho) = \frac{1}{2} \left[1 + \tanh \left(\frac{\rho - \rho_{acc}}{\Delta\rho} \right) \right] \quad (8)$$

- II. In the gap control mode the desired constant time gap T^* is imposed through its corresponding effect on a desired density ρ^* , defined as:

$$\rho^* = \frac{1}{1/\rho_{max} + T^*u^*} \quad (9)$$

The denominator in equation above is the desired space headway, in which $1/\rho_{max}$ reflects the vehicle's length $u^* = u(x^*)$ is the speed of the leading vehicle, computed at the "interaction" position:

$$x^* = x + \gamma^*(1/\rho_{max} + T^* \cdot u), \quad \gamma^* \in [1, 2] \quad (10)$$

Furthermore, after a relaxation time τ^* the speed relaxes to the speed of the leading vehicle u^* . Accordingly, the source term of Equation (2) that reflects the behavior of ACC vehicles can be expressed mathematically as

$$V_{acc}(\rho, u, \rho^*, u^*) = \frac{1}{2} \left[1 + \tanh \left(\frac{\rho - \rho_{acc}}{\Delta\rho} \right) \right] \left(\frac{\rho^* u^* - \rho u}{\tau^*} \right) \quad (11)$$

In [ISO 15622, 2010] it is recommended that for ACC systems indicated values should be $T^* \in [0.8, 2.2]$ s, while $\tau^* \approx 1$ s.

3. LINEAR STABILITY ANALYSIS FOR ACC SYSTEMS

Inherently, the stability analysis methods relate to the study of solutions and trajectories of a dynamical system with respect to introduced perturbations in the initial conditions. Regarding traffic flow theory, the response of drivers to a sudden stimulus, such as an abrupt deceleration or acceleration, results in the formation of disturbances that propagate in the traffic flow. Hence, the objective is to define the conditions under which the trajectories in case of microscopic models or the traffic state in

case of macroscopic ones remain stable with respect to appropriate introduced perturbation [16].

Towards this direction, this section aims to investigate the qualitative properties of the developed macroscopic model to reflect the effects of ACC-equipped vehicles on traffic flow stability. In order to do so, a proper stability condition for small perturbations will be derived, based on a linear stability method, which refers to linear Taylor approximations, used throughout the analysis. Linear stability analysis is a widely established approach to estimate the stability performance of the systems controlling the traffic flow. The consequence of using such linear approximations is that even if the traffic system is linearly stable, might actually still display nonlinear instability with respect to large perturbations. Thus, it should be highlighted that the aforementioned linear stability method is valid only in cases of small perturbations, since the method ignores higher order terms. When the magnitude of the perturbations is fairly large (caused, e.g., by hard braking maneuvers or inconsiderate lane changes), the linearization method might lead to incorrect results, as pointed out in [64]. Therefore, it is necessary to adopt other (nonlinear) techniques to derive the stability conditions under large perturbations, such as the wavefront expansion technique [50]. However, in general the linear analysis provides a valuable insight into the general behavior and performance of the model in the presence of ACC vehicles [30, 51].

The linear stability analysis starts supposing that the stationary and spatially homogeneous (i.e. time- and space-independent) solution of the system of partial differential Equations (1) and (2) are the constant density ρ_0 and corresponding speed u_0 [16, 23] Then, we consider small perturbations around the homogenous and stationary solution pair $(\rho_0$ and $u_0)$, denoted by $\delta\rho(x, t)$ and $\delta u(x, t)$:

$$\delta\rho(x, t) = \rho(x, t) - \rho_0 \text{ and } \delta u(x, t) = u(x, t) - u_0 \quad (12)$$

The essence of the stability analysis is to find the conditions under which the amplitude of the perturbations $\delta\rho(x, t)$ and $\delta u(x, t)$ diminishes, in order to gradually restore the equilibrium state.

Substituting $\rho(x, t) = \rho_0 + \delta\rho(x, t)$ and $u(x, t) = u_0 + \delta u(x, t)$ into the continuity Equation (1), using linear Taylor approximations, and neglecting nonlinear terms because of the assumption of small deviations $\delta\rho(x, t)/\rho_0 \ll 1$ and $\delta u(x, t)/u_0 \ll 1$ we obtain the following linearized equation:

$$\frac{\partial \delta\rho}{\partial t} + u_0 \frac{\partial \delta\rho}{\partial x} + \rho_0 \frac{\partial \delta u}{\partial x} = 0 \quad (13)$$

Analogously, the linearized equation for the momentum dynamics Equation (2), taking into account only the case of ACC vehicles, is transformed as

$$\frac{\partial \delta u}{\partial t} + u_0 \frac{\partial \delta u}{\partial x} + \frac{1}{\rho_0} \left[\frac{\partial P}{\partial u} \frac{\partial \delta u}{\partial x} + \frac{\partial P}{\partial \rho} \frac{\partial \delta \rho}{\partial x} \right] - \quad (14)$$

$$\frac{1}{\rho_0 \tau^*} \left[\frac{\partial(\rho^* u^*)}{\partial \rho} \delta \rho + \frac{\partial(\rho^* u^*)}{\partial u} \delta u - u_0 \delta \rho \right] + \frac{\delta u}{\tau^*} = 0$$

Accordingly, the form of the perturbed initial conditions must be chosen in a way that the stability analysis to be as general as possible. Actually, any functional form is possible to be applied for the perturbations $\delta \rho$ and δu . However, according to Fourier theory, any function can be decomposed into an infinite sum (or integral in cases of non-periodic functions) of sines and cosines. If the model is stable with respect to any sine or cosine function, it will be stable for any linear combination of these functions as well. Hence, proving the stability conditions of the model with respect to sine or cosine perturbations, also proves the general stability conditions to any functional form of the perturbations [23]. Consequently, we consider the following deviations:

$$\delta \rho(x, t) = \delta \rho_0 e^{\lambda t + i \omega x} \quad (15)$$

$$\delta u(x, t) = \delta u_0 e^{\lambda t + i \omega x} \quad (16)$$

where frequency λ and wave number ω are complex numbers: $\lambda, \omega \in \mathbb{C}$, i denotes the imaginary unit, and $\delta \rho_0$ and δu_0 are constants.

The remainder of the linear stability method concentrates on finding the conditions so as two restrictions are met [16, 23]:

- the deviation pair $\delta \rho(x, t)$ and $\delta u(x, t)$ is a solution of the model and
- this solution is stable, namely the amplitude of the perturbation is decreasing with time; this is true if the real part of frequency λ is strictly negative.

In order to satisfy the former condition we substitute the definitions for the perturbations $\delta \rho(x, t)$ and $\delta u(x, t)$ (Equations (15) and (16)) in the linearized Equations (13) and (14), which yields the following linear system

$$\underbrace{\begin{pmatrix} \lambda - a_{11} & a_{12} \\ a_{21} & \lambda - a_{22} \end{pmatrix}}_J \begin{pmatrix} \delta \rho_0 \\ \delta u_0 \end{pmatrix} = 0 \quad (17)$$

where

$$a_{11} = -i \omega u_0 \quad (18)$$

$$a_{12} = i \omega \rho_0 \quad (19)$$

$$a_{21} = i \omega \frac{1}{\rho_0} \frac{\partial P}{\partial \rho} - \frac{1}{\rho_0 \tau^*} \frac{\partial(\rho^* u^*)}{\partial \rho} \quad (20)$$

$$a_{22} = -i \omega \left(u_0 + \frac{1}{\rho_0} \frac{\partial P}{\partial u} \right) + \frac{1}{\rho_0 \tau^*} \frac{\partial(\rho^* u^*)}{\partial u} - \frac{1}{\tau^*} \quad (21)$$

This linear system has solutions other than the trivial solution $\delta \rho_0 = \delta u_0 = 0$, if and only if the determinant of the *Jacobian* matrix J is zero, that is

$$\det(J) = 0 \Leftrightarrow$$

$$\lambda^2 - (a_{11} + a_{22})\lambda + (a_{11}a_{22} - a_{12}a_{21}) = 0 \quad (22)$$

which results in

$$\lambda_1 = 0.5 \left(a_{11} + a_{22} + \sqrt{(a_{11} - a_{22})^2 + 4a_{12}a_{21}} \right) \quad (23)$$

$$\lambda_2 = 0.5 \left(a_{11} + a_{22} - \sqrt{(a_{11} - a_{22})^2 + 4a_{12}a_{21}} \right) \quad (24)$$

The latter condition is strictly fulfilled if the real part of the values of λ that obey $\det(J) = 0$ is strictly negative: $Real(\lambda_{1,2}) < 0$. Thus, we have

$$Real(a_{11} + a_{22}) = \frac{1}{\rho_0 \tau^*} \frac{\partial(\rho^* u^*)}{\partial u} - \frac{1}{\tau^*} \quad (25)$$

while, owing to the fact that the square root of Equations (23) and (24) contains a complex number we apply the following useful formula for separating the real part R and imaginary part I that is derived analytically in the Appendix:

$$\begin{aligned} \sqrt{R \pm |I|} &= \sqrt{0.5 \left(\sqrt{R^2 + I^2} + R \right)} \\ &\pm i \sqrt{0.5 \left(\sqrt{R^2 + I^2} - R \right)} \end{aligned} \quad (26)$$

This eventually results in

$$Real \left(\sqrt{(a_{11} - a_{22})^2 + 4a_{12}a_{21}} \right) = \sqrt{0.5 \left(\sqrt{R^2 + I^2} + R \right)} \quad (27)$$

with

$$R = \frac{1}{\tau^*} \left(1 - \frac{1}{\rho_0} \frac{\partial(\rho^* u^*)}{\partial u} \right)^2 - \left(\frac{\omega}{\rho_0} \frac{\partial P}{\partial u} \right)^2 - 4\omega^2 \frac{\partial P}{\partial \rho} \quad (28)$$

$$I = \frac{2\omega}{\rho_0 \tau^*} \frac{\partial P}{\partial u} \left(1 - \frac{1}{\rho_0} \frac{\partial(\rho^* u^*)}{\partial u} \right) - \frac{4\omega}{\tau^*} \frac{\partial(\rho^* u^*)}{\partial \rho} \quad (29)$$

Thus, from Equations (25) and (27), inequality $Real(\lambda_{1,2}) < 0$ results in:

$$\begin{aligned} \frac{1}{\rho_0 \tau^*} \frac{\partial(\rho^* u^*)}{\partial u} - \frac{1}{\tau^*} &< -\sqrt{0.5 \left(\sqrt{R^2 + I^2} + R \right)} \Leftrightarrow \\ \left(\frac{1}{\rho_0 \tau^*} \frac{\partial(\rho^* u^*)}{\partial u} - \frac{1}{\tau^*} \right)^2 &> 0.5 \left(\sqrt{R^2 + I^2} + R \right) \Leftrightarrow \end{aligned} \quad (30)$$

$$4 \left(\frac{1}{\rho_0 \tau^*} \frac{\partial(\rho^* u^*)}{\partial u} - \frac{1}{\tau^*} \right)^4 -$$

$$4 \left(\frac{1}{\rho_0 \tau^*} \frac{\partial(\rho^* u^*)}{\partial u} - \frac{1}{\tau^*} \right)^2 R > I^2 \Leftrightarrow$$

$$\frac{\partial P}{\partial \rho} \left(1 - \frac{1}{\rho_0} \frac{\partial(\rho^* u^*)}{\partial u} \right)^2 > \left(\frac{\partial(\rho^* u^*)}{\partial u} \right)^2$$

After an intermediate algebraic calculation, we end up with the following inequality

$$B \left(1 - \frac{1}{\rho_0} \mathcal{A} \right)^2 > \mathcal{A}^2 \Leftrightarrow$$

$$(B - \mathcal{A}^2) \rho_0^2 - 2B\mathcal{A}\rho_0 + B\mathcal{A}^2 > 0$$
(31)

where $B = \frac{\partial P}{\partial \rho}$, $\mathcal{A} = \frac{\rho_{max}}{(1+T^*\rho_{max}u)^2}$ and $B - \mathcal{A}^2 > 0$. Finding the zeroes from the last inequality, which are $\rho_{0,1,2} = \frac{\mathcal{A}B \pm \sqrt{B}\mathcal{A}^2}{B - \mathcal{A}^2}$, we conclude that the ACC system is stable if $\rho_0 > \frac{\mathcal{A}B + \sqrt{B}\mathcal{A}^2}{B - \mathcal{A}^2}$ and $\rho_0 < \frac{\mathcal{A}B - \sqrt{B}\mathcal{A}^2}{B - \mathcal{A}^2}$. As the term \mathcal{A}^2 is very small, we can simplify the denominator, and then the instability region is placed between $\mathcal{A} \pm \frac{\mathcal{A}^2}{\sqrt{B}}$. The center of the instability region is \mathcal{A} . For smaller values of T^* , \mathcal{A} becomes larger and as T^* tends to 0, \mathcal{A} tends to ρ_{max} . Consequently, by reducing ACC time-gap setting T^* , the instability region moves to higher values of density. Figure 1 contains the effect of T^* on the value of \mathcal{A} , using the velocity u as a parameter, while $\rho_{max} = 0.16 \frac{veh}{m}$.

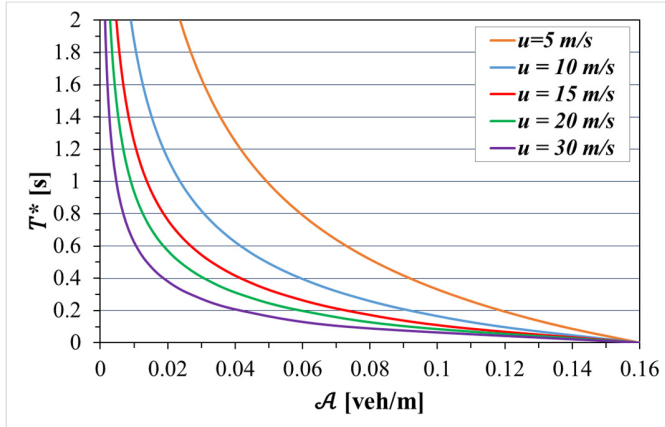


Fig. 1: Variation of \mathcal{A} with respect to time-gap setting T^* for $\rho_{max} = 0.16 \frac{veh}{m}$.

Referring to Fig. 1, for values of u greater-equal to 10 m/s and having a time-gap value around 1 s, the center \mathcal{A} of the instability region results at densities lower than the critical one,

where ACC is not active. Furthermore, the width $2 \frac{\mathcal{A}^2}{\sqrt{B}}$ of the instability region is less than $O(10^{-2})$ and decreases rapidly as velocity increases.

4. CONCLUSIONS

In this work a linear stability analysis was used to derive the stability region of a novel second-order macroscopic model of ACC traffic. The model is actually an extension of the GKT model, where the behavior of ACC-equipped vehicles is simulated by adding a proper source term to the momentum equation of the GKT model. This term was developed in order to satisfy the time/space-gap principle of ACC systems. The linear stability analysis revealed that the instability region is very narrow and is affected by the value of the selected ACC time-gap setting. For smaller values of the time-gap setting the instability region moves at higher values of density.

ACKNOWLEDGEMENTS

This research was supported by TRAFFIC MANAGEMENT for the 21st century (TRAMAN21) ERC Advanced Investigator Grand under the European Union's Seventh Framework Programme (FP/2007-2013).

REFERENCES

- [1] Zhou, J., and Peng, H., 2005, "Range policy of adaptive cruise control vehicles for improved flow stability and string stability," *IEEE Trans. Intell. Transp. Syst.*, **6**(2), pp. 229–237.
- [2] Herman, R., Montroll, E. W., Potts, R. B., and Rothery, R. W., 1959, "Traffic Dynamics: Analysis of Stability in Car Following," *Oper. Res.*, **7**(1), pp. 86–106.
- [3] Wilson, R. E., Berg, P., Hooper, S., and Lunt, G., 2004, "Many-neighbour interaction and non-locality in traffic models," *Eur. Phys. J. B*, **39**(3), pp. 397–408.
- [4] Treiber, M., Kesting, A., and Helbing, D., 2006, "Delays, inaccuracies and anticipation in microscopic traffic models," *Phys. Stat. Mech. Its Appl.*, **360**(1), pp. 71–88.
- [5] Kesting, A., and Treiber, M., 2008, "How reaction time, update time, and adaptation time influence the stability of traffic flow," *Comput.-Aided Civ. Infrastruct. Eng.*, **23**(2) pp. 125–137.
- [6] Yu, L., Shi, Z., and Zhou, B., 2008, "Kink–antikink density wave of an extended car-following model in a cooperative driving system," *Commun. Nonlinear Sci. Numer. Simul.*, **13**(10), pp. 2167–2176.
- [7] Li, X., Li, Z., Han, X., and Dai, S., 2009, "Effect of the optimal velocity function on traffic phase transitions in lattice hydrodynamic models," *Commun. Nonlinear Sci. Numer. Simul.*, **14**(5), pp. 2171–2177.
- [8] Zhang, P., Wong, S. C., and Dai, S. Q., 2009, "A conserved higher-order anisotropic traffic flow model: Description of equilibrium and non-equilibrium flows," *Transp. Res. Part B Methodol.*, **43**(5), pp. 562–574.
- [9] Tian, C., Sun, D., and Zhang, M., 2011, "Nonlinear analysis of lattice model with consideration of optimal current difference," *Commun. Nonlinear Sci. Numer. Simul.*, **16**(11), pp. 4524–4529.

- [10] Treiber, M., and Kesting, A., 2011, "Evidence of convective instability in congested traffic flow: A systematic empirical and theoretical investigation," *Transp. Res. Part B Methodol.*, **45**(9), pp. 1362–1377.
- [11] Peng, G., Nie, F., Cao, B., and Liu, C., 2011, "A driver's memory lattice model of traffic flow and its numerical simulation," *Nonlinear Dyn.*, **67**(3), pp. 1811–1815.
- [12] Tang, T., Wang, Y., Yang, X., and Wu, Y., 2012, "A new car-following model accounting for varying road condition," *Nonlinear Dyn.*, **70**(2), pp. 1397–1405.
- [13] Zheng, L.-J., Tian, C., Sun, D.-H., and Liu, W.-N., 2012, "A new car-following model with consideration of anticipation driving behavior," *Nonlinear Dyn.*, **70**(2), pp. 1205–1211.
- [14] Li, Y., Zhu, H., Cen, M., Li, Y., Li, R., and Sun, D., 2013, "On the stability analysis of microscopic traffic car-following model: a case study," *Nonlinear Dyn.*, **74**(1-2), pp. 335–343.
- [15] Ngoduy, D., 2013, "Analytical studies on the instabilities of heterogeneous intelligent traffic flow," *Commun. Nonlinear Sci. Numer. Simul.*, **18**(10), pp. 2699–2706.
- [16] Treiber, M., and Kesting, A., 2013, *Traffic Flow Dynamics: Data, Models and Simulation*, Springer Berlin Heidelberg.
- [17] Gupta, A. K., and Katiyar, V. K., 2005, "Analyses of shock waves and jams in traffic flow," *J. Phys. Math. Gen.*, **38**(19), pp. 4069–4083.
- [18] Tampere, C., Hoogendoorn, S., and van Arem, B., 2005, "A Behavioural Approach to Instability, Stop and Go Waves, Wide Jams and Capacity Drop," *Transp. Traffic Theory*, **16**, pp. 205–228.
- [19] Gupta, A. K., and Katiyar, V. K., 2006, "A new anisotropic continuum model for traffic flow," *Phys. Stat. Mech. Its Appl.*, **368**(2), pp. 551–559.
- [20] Zhang, P., and Wong, S. C., 2006, "Essence of conservation forms in the traveling wave solutions of higher-order traffic flow models," *Phys. Rev. E*, **74**(2).
- [21] Tang, T. Q., Huang, H. J., and Xu, G., 2008, "A new macro model with consideration of the traffic interruption probability," *Phys. Stat. Mech. Its Appl.*, **387**(27), pp. 6845–6856.
- [22] Ngoduy, D., and Tampere, C., 2009, "Macroscopic effects of reaction time on traffic flow characteristics," *Phys. Scr.*, **80**(2).
- [23] Helbing, D., and Johansson, A., 2009, "On the Controversy around Daganzo's Requiem for and Aw-Rasclé's Resurrection of Second-Order Traffic Flow Models," *Eur. Phys. J. B*, **69**(4), pp. 549–562.
- [24] Tang, T. Q., Li, C. Y., Wu, Y. H., and Huang, H. J., 2011, "Impact of the honk effect on the stability of traffic flow," *Phys. Stat. Mech. Its Appl.*, **390**(20), pp. 3362–3368.
- [25] Ngoduy, D., 2012, "Effect of driver behaviours on the formation and dissipation of traffic flow instabilities," *Nonlinear Dyn.*, **69**(3), pp. 969–975.
- [26] Ngoduy, D., 2013, "Platoon-based macroscopic model for intelligent traffic flow," *Transp. B Transp. Dyn.*, **1**(2), pp. 153–169.
- [27] Gupta, A. K., and Dhiman, I., 2014, "Analyses of a continuum traffic flow model for a nonlane-based system," *Int. J. Mod. Phys. C*, **25**(10).
- [28] Ngoduy, D., 2014, "Generalized macroscopic traffic model with time delay," *Nonlinear Dyn.*, **77**(1-2), pp. 289–296.
- [29] Ngoduy, D., and Wilson, R. E., 2014, "Multianticipative Nonlocal Macroscopic Traffic Model," *Comput.-Aided Civ. Infrastruct. Eng.*, **29**(4), pp. 248–263.
- [30] Swaroop, D., and Rajagopal, K. R., 1999, "Intelligent cruise control systems and traffic flow stability," *Transp. Res. Part C Emerg. Technol.*, **7**(6), pp. 329–352.
- [31] Alkim, T. P., Schuurman, H., and Tampere, C. M. J., 2000, "Effects of external cruise control and co-operative following on highways: an analysis with the MIXIC traffic simulation model," *Proc. IEEE Intelligent Vehicles Symposium IV*, pp. 474–479.
- [32] Marsden, G., McDonald, M., and Brackstone, M., 2001, "Towards an understanding of adaptive cruise control," *Transp. Res. Part C Emerg. Technol.*, **9**(1), pp. 33–51.
- [33] Davis, L. C., 2004, "Effect of adaptive cruise control systems on traffic flow," *Phys. Rev. E*, **69**(6).
- [34] Davis, L. C., 2007, "Effect of adaptive cruise control systems on mixed traffic flow near an on-ramp," *Phys. Stat. Mech. Its Appl.*, **379**(1), pp. 274–290.
- [35] Kesting, A., Treiber, M., Schönhof, M., Kranke, F., and Helbing, D., 2007, "Jam-Avoiding Adaptive Cruise Control (ACC) and its Impact on Traffic Dynamics," *Traffic and Granular Flow'05*, A. Schadschneider, T. Pöschel, R. Kühne, M. Schreckenberg, and D.E. Wolf, eds., Springer Berlin Heidelberg, pp. 633–643.
- [36] Kesting, A., Treiber, M., Schönhof, M., and Helbing, D., 2008, "Adaptive cruise control design for active congestion avoidance," *Transp. Res. Part C Emerg. Technol.*, **16**(6), pp. 668–683.
- [37] Kesting, A., Treiber, M., and Helbing, D., 2010, "Enhanced Intelligent Driver Model to Access the Impact of Driving Strategies on Traffic Capacity," *Philos. Trans. R. Soc. Math. Phys. Eng. Sci.*, **368**(1928), pp. 4585–4605.
- [38] Ntousakis, I. A., Nikolos, I. K., and Papageorgiou, M., 2014, "On microscopic modeling of Adaptive Cruise Control systems," *Proc. 4th International Symposium of Transport Simulation, Corsica, France*.
- [39] Sheikholeslam, S., and Desoer, C. A., 1992, "A System Level Study of the Longitudinal Control of a Platoon of Vehicles," *J. Dyn. Syst. Meas. Control*, **114**(2), pp. 286–292.
- [40] Ioannou, P. A., and Chien, C. C., 1993, "Autonomous intelligent cruise control," *IEEE Trans. Veh. Technol.*, **42**(4), pp. 657–672.
- [41] Swaroop, D., Hedrick, J. K., Chien, C. C., and Ioannou, P., 1994, "A Comparison of Spacing and Headway Control Laws for Automatically Controlled Vehicles1," *Veh. Syst. Dyn.*, **23**(1), pp. 597–625.
- [42] Swaroop, D., and Hedrick, J. K., 1996, "String stability of interconnected systems," *IEEE Trans. Autom. Control*, **41**(3), pp. 349–357.
- [43] Liang, C.-Y., and Peng, H., 1999, "Optimal Adaptive Cruise Control with Guaranteed String Stability," *Veh. Syst. Dyn.*, **32**(4-5), pp. 313–330.

[44] Liang, C.-Y., and Peng, H., 2000, "String Stability Analysis of Adaptive Cruise Controlled Vehicles," *JSME Int. J. Ser. C*, **43**(3), pp. 671–677.

[45] Treiber, M., and Helbing, D., 2002, "Microsimulations of Freeway Traffic Including Control Measures," *Automatisierungstechnik*, **49**(11), pp. 478–484.

[46] Li, P. Y., and Shrivastava, A., 2002, "Traffic flow stability induced by constant time headway policy for adaptive cruise control vehicles," *Transp. Res. Part C Emerg. Technol.*, **10**(4), pp. 275–301.

[47] Bareket, Z., Fancher, P. S., Peng, H., Lee, K., and Assaf, C. A., 2003, "Methodology for assessing adaptive cruise control behavior," *IEEE Trans. Intell. Transp. Syst.*, **4**(3), pp. 123–131.

[48] Yi, J., and Horowitz, R., 2006, "Macroscopic traffic flow propagation stability for adaptive cruise controlled vehicles," *Transp. Res. Part C Emerg. Technol.*, **14**(2), pp. 81–95.

[49] Demir, C., 2003, "Modelling the Impact of ACC-Systems on the Traffic Flow at Macroscopic Modelling Level," *Traffic and Granular Flow'01*, M. Fukui, Y. Sugiyama, M. Schreckenberg, and D.E. Wolf, eds., Springer Berlin Heidelberg, pp. 305–317.

[50] Yi, J., Lin, H., Alvarez, L., and Horowitz, R., 2003, "Stability of macroscopic traffic flow modeling through wavefront expansion," *Transp. Res. Part B Methodol.*, **37**(7), pp. 661–679.

[51] Ngoduy, D., 2012, "Application of gas-kinetic theory to modelling mixed traffic of manual and ACC vehicles," *Transportmetrica*, **8**(1), pp. 43–60.

[52] Ngoduy, D., 2013, "Instability of cooperative adaptive cruise control traffic flow: A macroscopic approach," *Commun. Nonlinear Sci. Numer. Simul.*, **18**(10), pp. 2838–2851.

[53] Treiber, M., Hennecke, A., and Helbing, D., 1999, "Derivation, properties, and simulation of a gas-kinetic-based, nonlocal traffic model," *Phys. Rev. E*, **59**(1), pp. 239–253.

[54] Helbing, D., Hennecke, A., Shvetsov, V., and Treiber, M., 2001, "MASTER: macroscopic traffic simulation based on a gas-kinetic, non-local traffic model," *Transp. Res. Part B Methodol.*, **35**(2), pp. 183–211.

[55] Treiber, M., Kesting, A., and Helbing, D., 2010, "Three-phase traffic theory and two-phase models with a fundamental diagram in the light of empirical stylized facts," *Transp. Res. Part B Methodol.*, **44**(8-9), pp. 983–1000.

[56] Helbing, D., 1997, "Modeling multi-lane traffic flow with queuing effects," *Phys. Stat. Mech. Its Appl.*, **242**(1–2), pp. 175–194.

[57] Ngoduy, D., 2006, "Derivation of Continuum Traffic Model for Weaving Sections on Freeways," *Transportmetrica*, **2**(3), pp. 199–222.

[58] Ngoduy, D., Hoogendoorn, S. P., and Liu, R., 2009, "Continuum modeling of cooperative traffic flow dynamics," *Phys. Stat. Mech. Its Appl.*, **388**(13), pp. 2705–2716.

[59] Helbing, D., and Treiber, M., 1998, "Gas-Kinetic-Based Traffic Model Explaining Observed Hysteretic Phase Transition," *Phys. Rev. Lett.*, **81**(14), pp. 3042–3045.

[60] Treiber, M., and Helbing, D., 1999, "Macroscopic simulation of widely scattered synchronized traffic states," *J. Phys. Math. Gen.*, **32**(1), pp. L17–L23.

[61] Helbing, D., and Treiber, M., 1999, "Numerical simulation of macroscopic traffic equations," *Comput. Sci. Eng.*, **1**(5), pp. 89–98.

[62] Delis, A. I., Nikolos, I. K., and Papageorgiou, M., 2014, "High-resolution numerical relaxation approximations to second-order macroscopic traffic flow models," *Transp. Res. Part C Emerg. Technol.*, **44**, pp. 318–349.

[63] Shladover, S., Su, D., and Lu, X.-Y., 2012, "Impacts of Cooperative Adaptive Cruise Control on Freeway Traffic Flow," *Transp. Res. Rec. J. Transp. Res. Board*, **2324**, pp. 63–70.

[64] Whitham, G. B., 1974, *Linear and Nonlinear Waves*, John Wiley & Sons.

APPENDIX

This section describes how to derive Equation (26) in order to recast the square root of a complex number. We start recalling that the set \mathbb{C} of complex numbers is formed by adding a square root i to the set of real numbers: $i^2 = -1$. Every complex number can be written as $R + iI$, where (R, I) are real numbers in Cartesian coordinates:

$$z = R + iI \quad (31)$$

In this case R denotes the real part of z , written as $R = Re(z)$ and I the imaginary part of z , written as $I = Im(z)$. In practice, the square roots of complex numbers can be easily found using the polar form. Hence, by switching to polar coordinates (r, θ) , the nonzero complex number z can be written in polar form as

$$z = r \cos(\theta) + ir \sin(\theta) \quad (32)$$

where $r \cos(\theta) = Re(z)$ and $r \sin(\theta) = Im(z)$ is the real and the imaginary part, respectively. The absolute value or modulus r is determined by

$$r = \sqrt{R^2 + I^2} = \sqrt{(R + iI)(R - iI)} = \sqrt{z\bar{z}} = |z| \quad (32)$$

where $\bar{z} = R - iI$ is the complex conjugate number, whereas the polar angle θ is defined as

$$\tan(\theta) = \frac{\sin(\theta)}{\cos(\theta)} = \frac{I}{R} = \frac{Im(z)}{Re(z)} \quad (33)$$

Next, using the Euler's formula

$$e^{i\theta} = \cos(\theta) + i \sin(\theta) \quad (34)$$

we can rewrite the aforementioned polar form of a complex number into its exponential form as follows

$$z = r[\cos(\theta) + i \sin(\theta)] = r e^{i\theta} \quad (35)$$

The exponential function can be defined on the complex plane by an infinite series expansion

$$\exp(z) = e^z = \sum_{n=0}^{\infty} \frac{z^n}{n!} \quad (36)$$

Therefore, the relationships for exponential functions are also applied to the case of complex numbers, getting the useful formulas for the product or quotient of complex numbers; i.e. the product of two complex numbers $z_1 = R_1 + iI_1 = r_1 e^{i\theta_1}$ and $z_2 = R_2 + iI_2 = r_2 e^{i\theta_2}$ is given by

$$\begin{aligned} z_1 z_2 &= (R_1 R_2 - I_1 I_2) + i(R_1 I_2 + I_1 R_2) = \\ &= r_1 e^{i\theta_1} r_2 e^{i\theta_2} = r_1 r_2 e^{i(\theta_1 + \theta_2)} = \\ &= r_1 r_2 \cos(\theta_1 + \theta_2) + i r_1 r_2 \sin(\theta_1 + \theta_2) \end{aligned} \quad (37)$$

Since the real and imaginary parts are linearly independent of each other, this yields that $R_1 R_2 - I_1 I_2 = r_1 r_2 \cos(\theta_1 + \theta_2)$ and $R_1 I_2 + I_1 R_2 = r_1 r_2 \sin(\theta_1 + \theta_2)$. Moreover, the inverse of any nonzero complex number is given by

$$\frac{1}{z} = \frac{1}{r e^{i\theta}} = \frac{e^{-i\theta}}{r} \quad (38)$$

where $i = \sqrt{-1} = e^{i\pi/2}$.

In general, the square of complex numbers in the form

$$z = r e^{\pm i\theta} = r[\cos(\theta) \pm i \sin(\theta)] \quad (39)$$

can be written either as

$$z^2 = r^2[\cos^2(\theta) \pm 2i \cos(\theta) \sin(\theta) - \sin^2(\theta)] \quad (40)$$

or, using the familiar additive property $e^{x_1} \cdot e^{x_2} = e^{x_1 + x_2}$ of the exponential function, as

$$\begin{aligned} z^2 &= r^2 (e^{\pm i\theta})^2 = r^2 e^{\pm i2\theta} = \\ &= r^2[\cos(2\theta) \pm i \sin(2\theta)] \end{aligned} \quad (41)$$

Thus, comparing the real parts and using the trigonometric identity $\cos^2(\theta) + \sin^2(\theta) = 1$, we have $\cos(2\theta) = 1 - 2 \sin^2(\theta) = 1 - 2[1 - \cos^2(\theta)] = 2 \cos^2(\theta) - 1$, from which the following trigonometric types are derived:

$$\cos^2(\theta/2) = \frac{1}{2}[1 + \cos(\theta)] \quad (42)$$

$$\sin^2(\theta/2) = \frac{1}{2}[1 - \cos(\theta)] \quad (43)$$

Consequently, the square root of a complex number is defined as

$$\begin{aligned} \sqrt{z} &= \sqrt{r} e^{\pm i\theta/2} = \sqrt{r}[\cos(\theta/2) \pm i \sin(\theta/2)] = \\ &= \sqrt{\frac{1}{2}[r + r \cos(\theta)]} \pm i \sqrt{\frac{1}{2}[r - r \cos(\theta)]} \end{aligned} \quad (44)$$

Taking into account that $R = r \cos(\theta)$ and $I = r \sin(\theta)$ we result to the following equation form:

$$\begin{aligned} \sqrt{R \pm iI} &= \\ &= \sqrt{\frac{1}{2}(\sqrt{R^2 + I^2} + R)} \pm i \sqrt{\frac{1}{2}(\sqrt{R^2 + I^2} - R)} \end{aligned} \quad (45)$$